Determination of inflationary observables by cosmic microwave background anisotropy experiments

Lloyd Knox*

Department of Physics, The University of Chicago, Chicago, Illinois 60637-1433
and NASA/Fermilab Astrophysics Center, Fermi National Accelerator Laboratory, Batavia, Illinois 60510-0500
(Received 3 April 1995)

Inflation produces nearly scale-invariant scalar and tensor perturbation spectra which lead to anisotropy in the cosmic microwave background (CMB). The amplitudes and shapes of these spectra can be parametrized by Q_S^2, $r \equiv Q_T^2/Q_S^2$, n_S, and n_T where Q_S^2 and Q_T^2 are the scalar and tensor contributions to the square of the CMB quadrupole and n_S and n_T are the power-law spectral indices. Even if we restrict ourselves to information from angles greater than one-third of a degree, three of these observables can be measured with some precision. The combination $105^{1-n_S}Q_S^2$ can be known to better than $\pm 0.3\%$. The scalar index n_S can be determined to better than ± 0.02. The ratio r can be known to about ± 0.1 for $n_S \simeq 1$ and slightly better for smaller n_S. The precision with which n_T can be measured depends weakly on n_S and strongly on r. For $n_S \simeq 1$, n_T can be determined with a precision of about $\pm 0.056(1.5+r)/r$. A full-sky experiment with a 20 arc min beam using technology available today, similar to those being planned by several groups, can achieve the above precision. Good angular resolution is more important than high signal-to-noise ratio; for a given detector sensitivity and observing time a smaller beam provides more information than a larger beam. The uncertainties in n_S and r are roughly proportional to the beam size. We briefly discuss the effects of uncertainty in the Hubble constant, baryon density, cosmological constant, and ionization history.

PACS number(s): 98.80.Cq, 98.70.Vc, 98.80.Es

I. INTRODUCTION

The detection of anisotropy of the cosmic microwave background (CMB) by the Cosmic Background Explorer (COBE) Differential Microwave Radiometer (DMR) [1] marks the beginning of a new era in observational cosmology. At least eight other experiments have subsequently made detections at angular scales ranging from 0.5° to a few degrees [2]. The many possible sources of systematic error combined with the fact that most of the results are not much better than 3σ detections mean that care must be used in drawing conclusions from them [3]. However, it is encouraging that they are roughly consistent with each other and that several experiments have reproduced their results with repeated observations of the same area of the sky. The results are consistent with a nearly scale-invariant spectrum, possibly with a feature at angular scales corresponding to the sound horizon at last scattering (the "Doppler peak") [4,5].

The current experiments, if not ruling out any theories with high confidence, are at the least providing strong constraints. For example, combined with large-scale structure data, the COBE DMR 2-yr data present a significant challenge to the primeval isocurvature baryon model [6,7] and imply large bias factors for defect models [8].

In addition to testing theories, the microwave background also provides us with the opportunity to determine the parameters of a given theory. For example,

in the cold dark matter (CDM) model the anisotropy depends on the amplitudes and slopes of the scalar and tensor spectra, the Hubble constant $H_0 = 100h$ km/sec Mpc, the baryon density $\Omega_b h^2$, the cosmological constant in units of the critical density Ω_Λ, and the redshift of reionization z_R. Bond *et al.* [9] have shown that, unfortunately, different choices of these parameters can lead to angular-power spectra which are indistinguishable by the current generation of experiments. This degeneracy makes it difficult to use CMB anisotropy experiments to determine cosmological parameters and hence the authors of [9] refer to the effect as "cosmic confusion." The degeneracy has a positive effect as well. It limits the space of possible power spectra, rendering the model testable despite its dependence on imprecisely known parameters [10,11].

The long-term goals of the CMB observational community are much more aggressive than those of the current generation of experiments [12]. As a partial step toward those goals several groups in the United States and Europe are currently planning a "next generation" satellite experiment. Using detector technology available today, such an experiment could sample the entire sky with a half-degree beam and in one year achieve a signal-to-noise ratio per beam-size pixel greater than one. Preliminary work by Spergel [13] indicates that such an experiment is sufficient for a significant lifting of the degeneracy of the angular-power spectrum pointed out by Bond *et al.*, at least in some regions of parameter space.

Here we are interested in what a "next generation" satellite could tell us about inflation in particular. In addition to resolving several cosmological puzzles, inflation is at the heart of the CDM scenario. In this picture,

---

*Current address: CITA, McLennan Labs, University of Toronto, 60 St. George Street, Toronto, ON, Canada M5S 1A1.

     52   4307

tensor, vector, and scalar fluctuations in the metric are produced during an early epoch of rapid expansion driven by the vacuum energy of a scalar field [14]. The scalar perturbations grow via gravitational instability into the variety of structures we observe in the Universe today, as well as producing CMB anisotropy from about 10 arc min scales up to the quadrupole. Vector perturbations decay with expansion and are of no phenomenological importance. The tensor perturbations today correspond to a stochastic background of gravity waves and also produce anisotropy in the microwave background at large angular scales ($\gtrsim 1°$).

Although there is no standard model of inflation, we can expect the spectra to have certain generic features. For inflation to occur, the dominant contribution to the energy density must be the vacuum energy of the scalar field. The kinetic energy is small in comparison, and hence the value of the scalar field changes slowly. Since the scalar field changes slowly while the Universe is rapidly expanding, the perturbation spectra are nearly scale invariant. Thus the power spectra are well approximated by power laws with spectral indices close to the Harrison-Zel'dovich values. To be more precise, the primordial power spectra over the length scales of astrophysical interest at some time deep in the radiation-dominated era are well approximated by the following power laws in comoving wave number k:

$$P_S(k) = A_S k^{n_S} ,$$
$$P_T(k) = A_T k^{n_T - 3} \qquad (1)$$

with $n_T \approx n_S - 1 \approx 0$. As an example, the spectra from $\lambda\phi^4$ chaotic inflation [15] are best fit by $n_S = 0.94$ and $n_T = -0.04$. The fit is good to about 1% in power from the quadrupole to the 10 arc min scale [16].

Since the two perturbation spectra are fit well by power laws, they can be characterized by four independent observables. We take them to be Q_S^2, $r \equiv Q_T^2/Q_S^2$, n_S, and n_T, where Q_S^2 and Q_T^2 are the expectation values of the scalar and tensor contributions to the square of the quadrupole. The quantities Q_S^2 and Q_T^2 should not be confused with the actual quadrupole moments on the sky which we can take to be the real parts of the spherical harmonic coefficients a_{22}, a_{21}, $a_{20}/\sqrt{2}$ and the imaginary parts of $a_{2,-1}$ and $a_{2,-2}$. The moments are related to Q_S^2 and Q_T^2 in the same way that events from a random process are related to their parent distribution. If the perturbations are Gaussian (which is almost certainly the case for inflation), each of the five quadrupole moments on the sky is a single realization drawn from a Gaussian distribution with zero mean and variance $\frac{2\pi}{5}(Q_S^2 + Q_T^2)$.

We wish to see how well these four inflationary observables can be determined from a satellite experiment. The extent to which the other parameters $(H_0, \Omega_b h^2, \ldots)$ can be determined as well remains an open question. Conceivably, their confusing effects may be detrimental to the precision with which the inflationary observables can be determined. We must remember, though, that we have other sources of information on the cosmological parameters. Observations of light element abundances constrain $\Omega_b h^2$ to be within the approximate range 0.009-

0.022 [17], a range which might well decrease to ±10% in the next few years by the deuterium abundance measurements made in quasar absorption line systems [18]. The Hubble Space Telescope key project of calibrating Cepheids [19] and several physics-based methods [20] promise to make a definitive measurement of the Hubble constant in the near future to ±5%. Polarization of the CMB can provide constraints on ionization history [21]. Gravitational lens statistics constrain the value of a cosmological constant [22]. Thus in the following, we take specific values for the cosmological parameters and assume that they are perfectly known. Later we discuss how well they must be known in order that the uncertainty be negligible.

It is worth pointing out that while the cosmological parameters may be determined by means other than CMB anisotropy, no observations are better suited to determining the primordial spectra. Redshift surveys will continue to be plagued by theoretical uncertainties in the relationship of mass to light (the so-called bias), hampering determination of n_S. Millisecond pulsars and space-based gravity wave detectors are probably not capable of detecting the very weak stochastic background of gravity waves expected from inflation, at least not in the near future [23,24].

To simulate experiments, we need to assume particular values not only of cosmological parameters, but of Q_S^2, n_S, n_T, and r as well. Below we focus on one case and then discuss how our results might change if the actual values are different. For the cosmological parameters we choose $h = 0.5$, $\Omega_\Lambda = 0$, $\Omega_b h^2 = 0.0125$ and the standard ionization history. For our theory of inflation we take the simplest model there is, chaotic inflation with a ϕ^4 potential. In addition to $n_S = 0.94$ and $n_T = -0.04$, chaotic inflation predicts $r = 0.28$. This is an example of a general rule for inflationary models called the consistency relation[1] $r = -7n_T$. To choose Q_S we note that for $n_S = 1$ and $r = 0$, the COBE DMR constrains the expectation value of the quadrupole to be $Q_S = 19.9 \pm 1.5$ μK [26]. Although the constraint would be slightly different for $n_S = 0.94$ and $r = 0.28$, our only concern here is for rough agreement; we simply take $Q_S = 20$ μK. Chaotic inflation is an attractive choice for this study not only for its simplicity but also because r is twice as large as it has to be to ensure its detectability [27].

In Sec. II, we describe our calculation methods. We discuss the calculation of the tensor and scalar angular-power spectra, and our modeling of experiments. In Sec. III, we show the results of attempts to recover Q_S, r, and n_S from simulated experiments with varying beam sizes and signal-to-noise ratios. In Sec. IV, we see how well the consistency relation can be tested by attempting to recover all four of the observables. In Sec. V, we consider how our results would change if we had assumed different input values of the inflationary observables and

---

[1]This relationship, which is accurate to lowest order in $(n_S - 1)$ and n_T, holds generally for slow-roll models; in some models $(n_S - 1) \simeq n_T$ and the stronger relation, $r = -7(n_S - 1)$, also holds; see Ref. [25].

cosmological parameters. Particular attention is paid to the effect of a cosmological constant on the consistency relation. In Sec. VI, we briefly examine the effects of uncertainty in cosmological parameters. Here we are interested in learning how well we have to know H_0, $\Omega_b h^2$, Ω_Λ, and reionization redshift z_R, so that our ignorance has a negligible effect on the determination of the inflationary observables.

II. CALCULATION METHODS

The spherical harmonics provide a convenient basis for the expansion of CMB-temperature fluctuations:

$$\delta T(\theta, \phi) = \sum_{l,m} a_{lm} Y_{lm}(\theta, \phi) . \qquad (2)$$

Isotropy in the mean guarantees that $\langle a_{lm} a^*_{l'm'} \rangle = C_l \delta_{ll'} \delta_{mm'}$, where angular brackets indicate an average over an ensemble of observers. It is the variance of the multipoles that encodes information about the metric perturbations and $C_l \equiv \langle a^2_{lm} \rangle$ is called the angular-power spectrum. (The expectation for the square of the quadrupole anisotropy is $Q^2 \equiv 5C_2/4\pi$.) Provided that the underlying perturbations are Gaussian, all predictions can be derived from the angular-power spectrum.

For example, the expected value of the variance of temperature fluctuations from a given experiment is given by

$$\langle \delta T^2 \rangle = \sum_l \frac{2l+1}{4\pi} C_l W_l , \qquad (3)$$

where the window function W_l depends on the beam size and chopping strategy. For example, an experiment that measures the temperature difference between directions separated by angle θ with beam size σ_b has a window function $W_l = [1 - P_l(\cos(\theta))]e^{-l^2\sigma_b^2}$. For a map made with a Gaussian beam, $W_l = e^{-l^2\sigma_b^2}$.

We calculate the angular-power spectra by numerically evolving the photon distribution function from deep in the radiation-dominated era until the present moment according to the first-order general relativistic Boltzmann equation for radiative transfer. Details are given elsewhere [28]. The results of one calculation are shown in Fig. 1.

To model the experiment, we assume that it creates a full-sky pixelized map of the CMB smoothed with a Gaussian beam with full width at half maximum θ_{FWHM}. The temperature of the ith pixel, δT_i, has a contribution from the sky and from the instrument noise: $\delta T_i = \delta T_i^{sky} + \delta T_i^{noise}$. We further assume that the errors are uncorrelated and have uniform variance σ^2_{pix}; i.e., $\langle \delta T_i^{noise} \delta T_j^{noise} \rangle = \sigma^2_{pix} \delta_{ij}$. For the moment we assume that $\delta T_i^{sky} = \delta T_i^{CMB}$, an assumption we will soon discard.

There are several different ways of describing the amount of noise in a map. The most straightforward way is to specify σ_{pix}. Another way is to specify the signal-to-noise ratio per pixel, S/N. The observing time per pixel
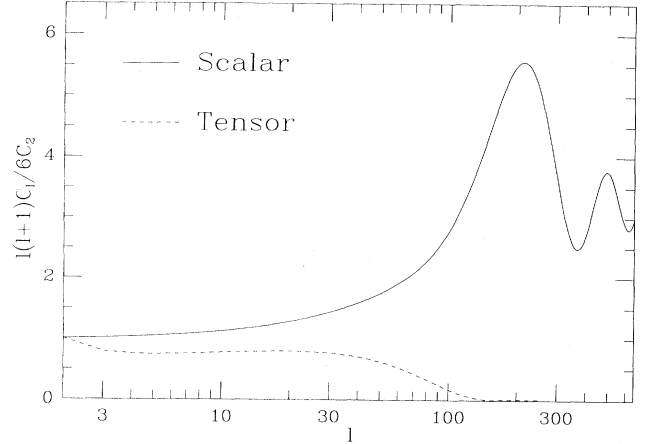
FIG. 1. Tensor and scalar angular-power spectra for $n_S = 1$ and $n_T = 0$.

is inversely proportional to the pixel size, so both σ_{pix} and S/N depend on the pixel size. For definiteness, whenever referring to S/N or σ_{pix}, we will take the pixel solid angle to be $\Omega_{pix} = \theta_{FWHM} \times \theta_{FWHM}$. To compare maps with different beam sizes, it is useful to have a measure of noise that is independent of Ω_{pix}. For that purpose we use the weight per solid angle, $w \equiv (\sigma^2_{pix} \Omega_{pix})^{-1}$.

The error in each pixel, σ_{pix}, depends on the detector sensitivity s and the time spent observing each pixel, t_{pix}: $\sigma_{pix} = s/\sqrt{t_{pix}}$. The best detectors available today have sensitivities on the order of 200 μK $\sqrt{sec}$. With uniform full-sky coverage over the course of a year every 20 arc min $\times$ 20 arc min pixel could be observed for 85 sec. Such a year of observing would result in a map with $\sigma_{pix} = 22\ \mu$K for $\Omega_{pix} = 20$ arc min $\times$ 20 arc min, or a weight per solid angle of $w = (7.5\ \mu\text{K})^{-2}$ deg^{-2}. For comparison, the 2-yr COBE maps have $w \simeq (400\ \mu\text{K})^{-2}$ deg^{-2}. The considerable difference between these numbers is due to the $\sim$ 70-fold improvement of detector sensitivities in the last 20 years.

The signal used to calculate S/N is the rms of the temperature fluctuations. The expected signal is given by Eq. (3). For the model we simulate here the expected signal with $\theta_{FWHM} = 20$ arc min is 92.5 μK. Therefore the case of $\sigma_{pix} = 22\ \mu$K has $S/N \simeq 4$.

In our simulations, we never create a map. Instead we exploit the fact that the estimate of C_l which could be made from such a map, C_l^{est}, would be χ^2_{2l+1} distributed with mean $\langle C_l^{est} \rangle = C_l$ and variance[2]

$$(\Delta C_l)^2 \equiv \langle (C_l^{est} - C_l)(C_{l'}^{est} - C_{l'}) \rangle$$
$$= \frac{2}{2l+1} (C_l + w^{-1}e^{l^2\sigma_b^2})^2 \delta_{ll'} \qquad (4)$$

---

[2]Equation (4) does not include any error due to finite pixelization. At moderate to low S/N, these errors are unimportant if the pixel size is a few times smaller than the beam size.

(see the Appendix). In the limit $w = \infty$ ($\sigma_{\mathrm{pix}} = 0$), $(\Delta C_l)^2$ does not go to zero. This is because the finite sampling of events from a random process always leads to an uncertainty in the variance, called sampling variance, no matter how precisely each event is measured. The sampling variance for a Gaussian distribution is equal to twice the square of the variance divided by the number of samples. For each l there are $2l+1$ "samples" drawn from a Gaussian distribution of variance C_l, hence the $2/(2l+1)$ factor in Eq. (4). In this limit of full-sky coverage, sampling variance is known as cosmic variance [29].

The signal at large l is reduced by the beam but the noise is not. If the beam profile is perfectly known, as is assumed here, one can take account of this diminution of signal by deconvolving the effect of the beam. The cost of doing so is the exponential factor in the noise term.

Equation (4) can be rewritten in a more illuminating manner:

$$\frac{\Delta C_l}{C_l} = \sqrt{\frac{2}{2l+1}} \left(1 + \frac{l^2 w^{-1}}{l^2 C_l} e^{l^2 \sigma_b^2}\right) . \qquad (5)$$

This form is useful because $l^2 C_l$ varies by less than an order of magnitude from $l = 2$ to $l \simeq 1000$ for the models we consider. The cosmic variance term is proportional to $1/\sqrt{l}$ and dominates at small l. The noise term is proportional to $l^{3/2}$ at small l and for $l \gtrsim 1/\sigma_b$ it increases exponentially.

In Fig. 2, we show $\Delta C_l/C_l$ for four experiments with two different beam sizes and two different values of w. One can see from the figure that, at constant w, the experiment with the better angular resolution is more precise at every value of l. The comparison at constant w is meaningful since these are experiments with the same detector sensitivity and observing time.

From Eq. (4) it is easy to show that reducing the beam size at fixed detector sensitivity and observing time re-

duces ΔC_l for every l, independent of C_l, as is evident in Fig. 2. At small values of l, ΔC_l is near the cosmic variance limit and thus decreasing the beam decreases ΔC_l only slightly. But for $l \gtrsim 1/\sigma_b$ the reduction in ΔC_l is dramatic. Thus there is much to be gained by reducing the size of the beam, even if this means reducing the signal-to-noise ratio to below unity.

To this point we have assumed that $\delta T_i^{\mathrm{CMB}} = \delta T_i^{\mathrm{sky}}$. However, synchrotron and bremsstrahlung radiation, thermal emission from cold dust, and unresolved extragalactic sources also contribute to the anisotropy of radiation at submillimeter to centimeter wavelengths at the angular scales of interest [30]. For this reason, a satellite experiment must make measurements over a range of wavelengths, so that the CMB component can be detected by its (hopefully) unique spectral dependence. Given σ_{pix} for a number of different frequencies, and guesses at the slopes and amplitudes of different contaminating sources, one can estimate $\sigma_{\mathrm{pix}}^{\mathrm{CMB}}$, the standard deviation in the determination of $\delta T_i^{\mathrm{CMB}}$ [31,32]. Preliminary design studies by the MAP collaboration indicate that the foregrounds will degrade the noise level by a factor of 2–3 [33]. Therefore, we take into account the effect of foreground contamination by simply decreasing w from $(7.5~\mu\mathrm{K})^{-2}~\mathrm{deg}^{-2}$ to $(15~\mu\mathrm{K})^{-2}~\mathrm{deg}^{-2}$ in one case and, to be conservative, $(30~\mu\mathrm{K})^{-2}~\mathrm{deg}^{-2}$ in another.[3]

Including the effects of foreground contamination makes the comparison of experiments with different beam sizes less straightforward. This is because the contamination may be more important at one angular scale than another and thus cause more degradation in a 40 arc min experiment than in a 20 arc min experiment. However, the smaller beam experiment will still always provide more information. As proof, we point out that it is always possible to synthesize a larger beam, after having done the experiment with a smaller beam. The interesting question becomes a quantitative one; how much better is a smaller beam? The answer depends on the spatial correlations of the contaminating sources, their frequency dependence and amplitudes, and the frequency coverage of the experiment. A complete investigation of this question is outside the scope of this paper. Here we only consider a very simple case of randomly distributed uniform point sources and an experiment that only measures at one frequency. For this case, the $\sqrt{N}$ fluctuations in the number of point sources, N, in a given pixel imply $\sigma_{\mathrm{pix}}^{\mathrm{CMB}} \propto 1/\Omega_{\mathrm{pix}}$. Thus for this case the comparison between different experiments should be made at equal weight per solid angle, just as for the no-foreground case.

We simulate an experiment by drawing C_l^{est} from the distribution in Eq. (4) and then estimate Q_S, n_S, and r from the "data" (the set of moments, $\{C_l^{\mathrm{est}}\}$) by finding the maximum of the likelihood function[4] $\mathcal{L}(Q_S, n_S, r)$.
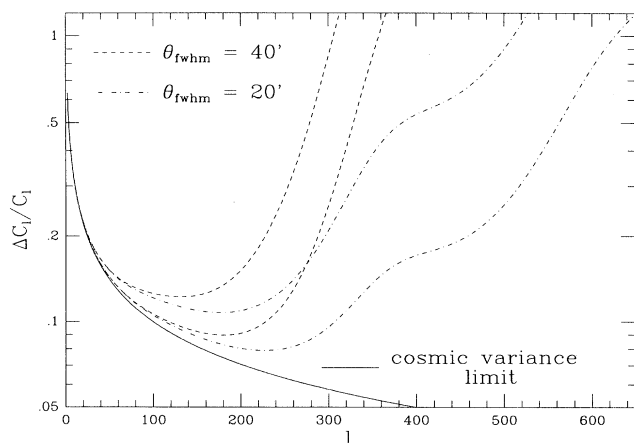
FIG. 2. The precision of four different experiments. The dashed lines are for experiments with $\theta_{\mathrm{FWHM}} = 40$ arc min and the dot-dashed lines are for experiments with $\theta_{\mathrm{FWHM}} = 20$ arc min. For each, the lower curve is for $w = (15~\mu\mathrm{K})^{-2}~\mathrm{deg}^{-2}$ and the upper is for $w = (30~\mu\mathrm{K})^{-2}~\mathrm{deg}^{-2}$.

---

[3]The removal of foregrounds will not only increase the noise level but also introduce correlations in the noise from one pixel to the next. We ignore this effect [34].

[4]Both the simulation and estimation procedures assume $r = -7n_T$.

The likelihood function is, up to a constant, independent of its arguments, defined as the probability density of measuring the set of moments C_l^{est} given $C_l(Q_S, n_S, r)$:

$$\mathcal{L}(Q_S, n_S, r) \propto P[C_l^{\text{est}} | C_l(Q_S, n_S, r)]$$

$$= \Pi_l \frac{n_l}{C_l + w^{-1} e^{l^2 \sigma_b^2}} \frac{V_l^{(n_l - 2)/2} \exp(-V_l/2)}{2^{n_l/2} \Gamma(n_l/2)} ,$$

where

$$V_l \equiv (2l + 1) \frac{C_l^{\text{est}} e^{-l^2 \sigma_b^2} + w^{-1}}{C_l e^{-l^2 \sigma_b^2} + w^{-1}} \qquad (6)$$

and $n_l \equiv 2l + 1$. The product on the right-hand side is simply that of the χ^2_{2l+1} distributions with mean C_l and variance given by Eq. (4) (see the Appendix).

To measure the certainty with which the observables can be determined we examine the distribution of the maxima from many simulations. An automated search, which uses the numerical technique of simulated annealing [35], finds the maximum for each set of simulated "data." Evaluation of the likelihood function on a fine grid of n_S, Q_S, and r shows that the maximum found by the automated procedure differs negligibly from the true maximum. Performing N simulations allows us to determine the standard deviations of the observables with a fractional statistical error of $(2N)^{-0.5}$. Typically we take $N = 100$ which gives about 7% accuracy.

III. RESULTS

Figure 3 shows the maxima projected into the Q_S-n_S plane from 100 simulations of an experiment with $\theta_{\text{FWHM}} = 20$ arc min and $w = (15 \ \mu\text{K})^{-2} \ \text{deg}^{-2}$. The average values of n_S and Q_S are equal to their input values to within 0.05% and hence there is no evidence for bias. The standard deviation in the values of n_S and Q_S are 0.016 and 0.74 μK, respectively. We can conclude then that an experiment of this type can determine n_S with
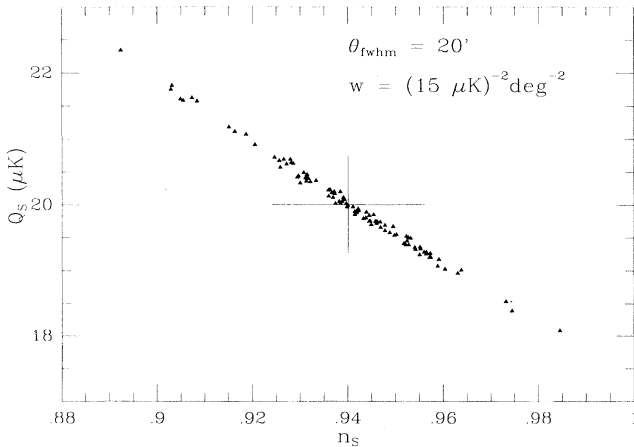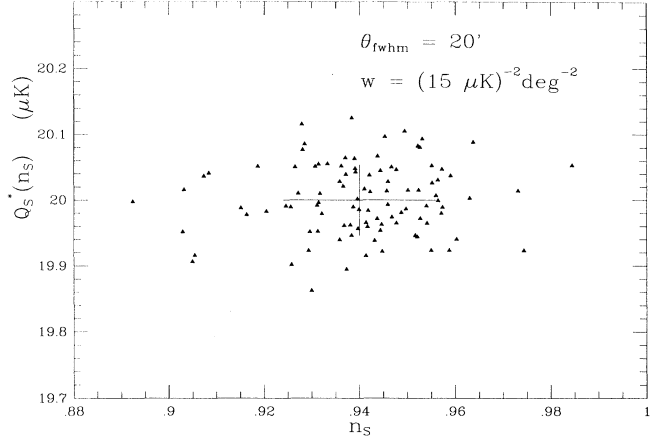
FIG. 4. The maxima of the likelihood functions for 100 simulations projected into the $Q_S^*(n_S)$-n_S plane (see text).

$\Delta n_S = 0.016 \pm 0.001$ and Q_S with $\Delta Q_S = (0.74 \pm 0.052)$ μK.

The strong correlation between Q_S and n_S, evident in Fig. 2, can be easily understood. It is due to the lever arm between $l = 2$ and those values of l, l^*, for which C_l is measured most precisely. If C_{l^*} were the only moment measured then $(Q_S, n_S) = (20 \ \mu\text{K}, 0.94)$ would fit the data as well as $(20 \ \mu\text{K}(l^*/2)^{(0.94-n_S)/2}, n_S)$ since each set of parameters results in nearly the same value of C_{l^*}. Keeping $Q_S \propto (l^*/2)^{-n_S/2}$ as n_S varies, causes the spectrum to "pivot" about l^* and thus we call l^* the pivot point of the data.

The combination $Q_S^*(n_S) \equiv \gamma Q_S (l^*/2)^{n_S/2}$ is uncorrelated with[5] n_S. We choose the proportionality constant to be $\gamma = (l^*/2)^{-0.94/2}$ so that the mean value of Q_S^* equals the mean value of Q_S. For the experiment under consideration, the pivot point is at $l^* = 210$. Figure 4 shows the same maxima as in Fig. 3, but in the new coordinates $n_S, Q_S^*(n_S)$. There is very little bias in the estimate of Q_S^*; the average value of Q_S^* is 20.001 μK. We find that $\Delta Q_S^*(n_S) = (0.0027 \pm 0.0002)$ μK.

For fixed $C_{l'}$, low Q_S and high n_S mean that the fit has too little power at small l. To make up this deficit, r is overestimated. Thus there is also a correlation between r and n_S (and hence Q_S), a correlation which is evident in Fig. 5. We find $\Delta r = 0.11 \pm 0.008$. There is very little bias; the average value of r is 0.29.

We have analyzed the results from simulated experiments with a range of beam sizes and S/N ratios. The results are shown in Fig. 6 and Table I. Each experiment has been simulated 100 times and thus the error bars are about the same size as the plotting symbols.

To some extent we can understand the numerical results with simple analytic arguments. First we will attempt to understand the precision with which the am-

FIG. 3. The locations of the maxima from 100 simulations are shown projected into the Q_S-n_S plane. The average values of n_S and Q_S, as well as their standard deviations, are indicated by the error bars.

---

[5]In fact, we find l^* by changing it until $Q_S^*(n_S)$ is uncorrelated with n_S.
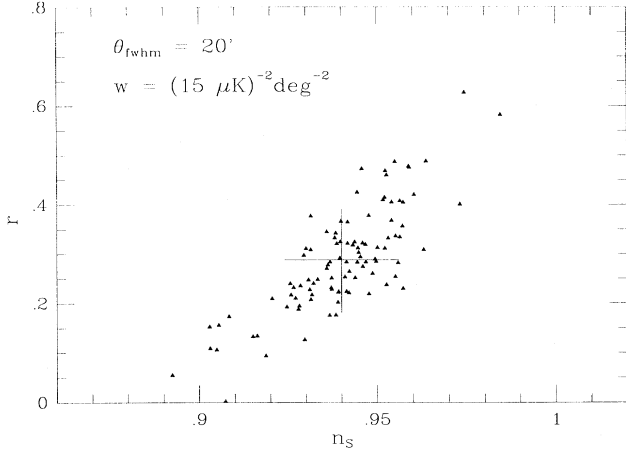
FIG. 5. The maxima of the likelihood functions for 100 different simulations projected into the r-n_S plane.

FIG. 6. The standard deviations of three of the four inflationary observables expected from experiments with three different beam sizes and two different weights per solid angle, w. Squares indicate Δr, triangles Δn_S, and pentagons $\Delta Q_S^*/Q_S^*$. The solid lines connect experiments with $w = (15 \ \mu\text{K})^{-2}$ deg^{-2}. Along the dashed lines, $w = (30 \ \mu\text{K})^{-2}$ deg^{-2}.

plitude can be determined. If the shape of the angular-power spectrum were perfectly known (C_l^{shape}) then each $C_l = \alpha^2 C_l^{\text{shape}}$ would be an independent measurement of the amplitude, α. A straightforward way to estimate α^2 is to take a weighted average of C_l/C_l^{shape} from some lower limit on l, $l_<$, to an upper limit, $l_>$. Thus we define

$$\alpha^2_{l_<,l_>} \equiv \sum_{l=l_<}^{l_>} \frac{C_l}{C_l^{\text{shape}}} \left(\frac{\Delta C_l}{C_l}\right)^{-2} \Bigg/ \sum_{l=l_<}^{l_>} \left(\frac{\Delta C_l}{C_l}\right)^{-2} \quad (7)$$

and we find

$$\frac{\Delta\alpha^2_{l_<,l_>}}{\alpha^2_{l_<,l_>}} = \left(\sum_{l=l_<}^{l_>} \left(\frac{\Delta C_l}{C_l}\right)^{-2}\right)^{-1/2}. \quad (8)$$

The numerical results for $\Delta Q_S^*/Q_S^*$ are reproduced to within about 10% by $\Delta\alpha_{2,\infty}/\alpha_{2,\infty} = 0.5\Delta(\alpha^2_{2,\infty})/(\alpha^2_{2,\infty})$. This agreement suggests that our

attempts to fit more than just an amplitude have not significantly degraded the quality of the amplitude measurement.

The effect of small changes in the scalar index n_S will be to make α a slowly varying function of l which we will now call α_l. Since the wave number k that contributes the most to any C_l is proportional to l, we have the approximate relation

$$\alpha^2_{l_1} \simeq \alpha^2_{l_2} \left(\frac{l_1}{l_2}\right)^{n_S-1}. \quad (9)$$

If we measure α_l in two different bands of l, say α_{2,l_B} and $\alpha_{l_B+1,\infty}$ then the resulting uncertainty in n_S is

$$\Delta n_S \simeq [\ln(l_C/l_B)]^{-1}\sqrt{\left(\frac{\Delta(\alpha^2_{2,l_B})}{\alpha^2_{2,l_B}}\right)^2 + \left(\frac{\Delta(\alpha^2_{l_B+1,\infty})}{\alpha^2_{l_B+1,\infty}}\right)^2}, \quad (10)$$

TABLE I. The precision with which the three independent inflationary observables can be measured.

θ_{FWHM} (arc min)	$\sqrt{1/w}$ [a]	l_C	l_B	$\Delta Q_S^*/Q_S^*$ [b]	$\Delta Q_S^*/Q_S^*$ [c]	Δn_S [b]	Δn_S [c]	Δr [b]	Δr [c]
20	15	227	85	0.0026	0.0027	0.017	0.016	0.10	0.11
20	30	175	60	0.0037	0.0041	0.023	0.029	0.13	0.18
30	15	205	70	0.0030	0.0028	0.020	0.022	0.11	0.14
30	30	156	55	0.0043	0.0047	0.026	0.044	0.16	0.23
40	15	181	65	0.0034	0.0035	0.023	0.034	0.15	0.19
40	30	131	50	0.0049	0.0050	0.029	0.058	0.18	0.42

[a] Units are (μK) deg.
[b] Analytic.
[c] Numerical.

where l_C is the value of l for which $\frac{\Delta C_l}{C_l}$ is a minimum. Choosing l_B to minimize Δn_S gives the results shown in Table I.

The analytic approximation to the amplitude results in Table I is given by $\Delta Q_S^*/Q_S^* = \Delta \alpha_{l_B+1,\infty}/\alpha_{l_B+1,\infty}$. These values are only a few percent larger than what we would get if the lower limit on the sum were $l = 2$. The difference between the numerical and analytic results for the amplitude is small enough to be completely explained by the $\sim 7\%$ statistical error.

For $l_B \leq 65$, the analytic results for Δn_S are systematically low. The primary reason for this is probably the confusing effect of having to fit for r as well. As l_B becomes less than about 65, a significant amount of the information used in determining Δn_S is also used for determining r. An encouraging result is that the analytic results for Δn_S work well for the two highest values of l_B, suggesting that the confusing effect of r on Δn_S vanishes with sufficiently high angular resolution and weight per solid angle.

With Q_S and n_S known the scalar spectrum is completely determined. Any excess power at $l \lesssim 65$ can therefore be ascribed to the influence of the gravity waves. Knox and Turner [27] showed that a specific window function, W_l^A, centered at $l_A \simeq 55$ is ideally suited for detecting this excess power. They used it to define an observable proportional to r:

$$Z_A \equiv \frac{\langle \delta T_A^2 \rangle}{\langle \delta T_A^2 \rangle_{\text{scalar}}} - 1 \,, \tag{11}$$

where $\langle \delta T_A^2 \rangle_{\text{scalar}} = \sum_l \frac{2l+1}{4\pi} C_l^S W_l^A$ is the anisotropy expected in experiment A from the scalar spectrum, which is fully determined by experiments B and C. If the proportionality constant α_A is such that $r = \alpha_A Z_A$ then

$$
\begin{aligned}
(\Delta r)^2 &= \alpha_A^2 (\Delta Z_A)^2 \\
&= \left(\alpha_A \frac{\Delta \langle \delta T_A^2 \rangle}{\langle \delta T_A^2 \rangle} \right)^2 + \left((\alpha_A + 4) \frac{\Delta \langle \delta T_A^2 \rangle_{\text{scalar}}}{\langle \delta T_A^2 \rangle_{\text{scalar}}} \right)^2 \\
&= \left(\frac{\alpha_A + r}{l_A} \right)^2 + [(\alpha_A + r)\Delta n_S \ln(l_C/l_A)]^2 \,. \tag{12}
\end{aligned}
$$

Let us concentrate first on the case $\Delta n_S = 0$, the one considered in [27]. The last expression follows from the approximation of W_l^A as a top hat centered at l_A with width l_A. Taking $\alpha_A = 3$ (since $C_{55}^T/C_{55}^S \simeq r/3$, from Fig. 1) we find $\Delta r = 0.055$ (for $r \ll \alpha_A$). Knox and Turner found $r_{\min} = 0.14$, where $r_{\min}$ is defined to be that value of r for which 95% of the time $r = 0$ can be ruled out with 95% confidence or greater. In order to compare results we must convert Δr to $r_{\min}$. Since the tail of a Gaussian containing 5% of the area is a distance 1.6σ from the maximum, $r_{\min} = 3.2 \times \Delta r$. Thus we find $r_{\min} = 0.17$, which compares fairly well with the exact result.

The last expression for the second term in Eq. (12) follows from the fact that the uncertainty in the scalar contribution to Z_A is entirely due to Δn_S and the lever arm between $l_A \simeq 55$ and l_C. The "analytic" results for Δr in Table I were calculated by substituting the

numerical values of Δn_S into Eq. (12). The agreement is good when the efforts to fit n_S and r do not rely on the same multipole moments but as l_B decreases, the agreement worsens.

IV. CONSISTENCY RELATION

As mentioned above, inflation predicts a relationship between the tensor amplitude to scalar amplitude ratio and the shape of the tensor spectrum. This relationship can be simply expressed in terms of the observables. To lowest order in the deviation from scale invariance it is $r = -7n_T$. If we could measure both r and n_T with precision, this relationship would provide a powerful test of inflation [25]. Unfortunately, the only effect of the gravity waves that we can hope to detect in the near future is the increased anisotropy of the microwave background at large angular scales. This limited range of length scales over which the tensor spectrum has an observable influence makes the measurement of n_T very difficult.

For large r the tensor spectrum stands out more relative to the scalar spectrum, thereby decreasing Δn_T. For this reason, and because we are pessimistic about the prospects for determining n_T well, we study the case $r = 1$, $n_T = -0.14$. For the same reason, decreasing n_S also decreases Δn_T, but not as dramatically. However, the combination of large r and $n_S \ll 1$ is strongly disfavored because it leaves insufficient power for structure formation on galactic scales. Therefore we choose to study $n_S = 1$.

In Fig. 7, the values of $r^*(n_T)$ and n_T are shown which maximize the likelihood functions of 200 simulated experiments with $\theta_{\text{FWHM}} = 20$ arc min, $w = (15 \ \mu\text{K})^{-2} \ \text{deg}^{-2}$. The combination $r^*(n_T) = r(l^*/2)^{n_T+0.14}$ is analogous to $Q_S^*(n_S)$ in the scalar case. We find the pivot point to be at $l^* = 20$ and $\Delta n_T = 0.14$.

The uncertainty in n_T can be understood by imagining amplitude measurements at a pair of angular scales, ex-
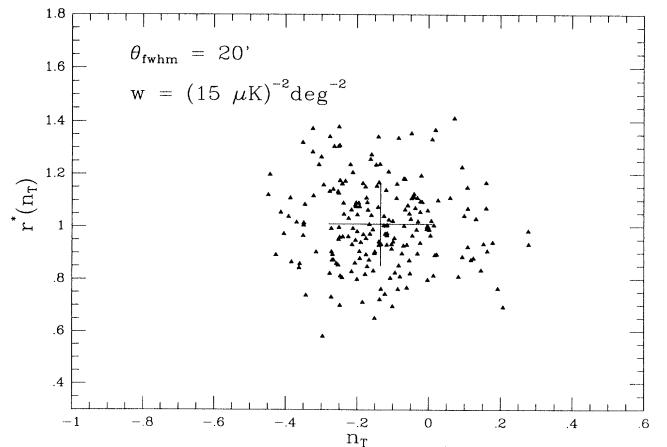
FIG. 7. The maxima of the likelihood function of 200 simulations projected into the $r^*(n_T)$-n_T plane (see text). The "data" were synthesized for $n_S = 1$, $Q_S = 20 \ \mu\text{K}$, $r = 1$, and $n_T = -\frac{1}{7}$. Unlike the previous cases n_T is not constrained to obey the consistency equation $r = -7n_T$.

actly as was done for the scalar case. Rewriting Eq. (10) for n_T,

$$(\Delta n_T)^2 \simeq [\ln(l_A/l_D)]^{-2}$$

$$\times \left(\left(\frac{\Delta Z_A}{Z_A} \right)^2 + \left(\frac{\Delta Z_D}{Z_D} \right)^2 \right) , \qquad (13)$$

where Z_D is defined analogously to Z_A. Equation (13) is correct only if we neglect the contributions to ΔZ_A and ΔZ_D that are due to uncertainty in n_S, since these contributions to the error in n_T nearly cancel each other. The value of l_D that minimizes Δn_T is about $l_A/3$. Since $l_A \simeq 55$, $l_D \simeq 18$. At this minimum,

$$\Delta n_T \simeq \left(\frac{\alpha_D + r}{r} \right) 0.056 . \qquad (14)$$

From Fig. 1 we see that $C_{18}^T/C_{18}^S \simeq r/1.5$. Therefore $\alpha_D \simeq 1.5$ and $\Delta n_T = 0.14$ for $r = 1$, in agreement with the numerical result.

Whether this precision allows for a test of inflation depends on the alternative hypotheses. For example, $n_T = -r/7$ and 0 are not necessarily distinguishable for $r \lesssim 1$. However, if there were a large deviation from scale invariance, say $n_T = 1$, then we would clearly be able to falsify the consistency relation, at least for $r \gtrsim 0.4$.

Higher-order corrections to the consistency relation are unlikely to be an important consideration in its testing. To second order in $n_S - 1$ and n_T, the consistency relation is [36]

$$n_T = -\frac{r}{7}[1 + 0.11r + 0.15(n_S - 1)] . \qquad (15)$$

Even for $r = 2$, the correction to the expected value of n_T is only about 0.03.

Measurement of the polarization of the microwave background provides another means of gaining information on the tensor perturbations. For $l \lesssim 10$, polarization of CBR anisotropy due to tensor perturbations is about $\sqrt{60r}$ times greater than that due to scalar perturbations [21]. However, the polarization-to-anisotropy ratio is less than 1% even for $r = 1-$ and polarization is difficult to measure on large angular scales. For the foreseeable future it is unlikely that polarization measurements will provide significant information on the tensor spectrum.

V. DEPENDENCE ON COSMOLOGICAL PARAMETERS

At fixed signal-to-noise ratio, the sensitivity of the above experiments to Q_S and n_S is nearly independent of the actual values of h, Ω_b, Ω_Λ, and n_S. However, Ω_Λ and n_S do affect the sensitivities to r and n_T through their effect on the shape of the scalar spectrum for $l \lesssim 60$. For example, decreasing n_S at fixed r increases C_l^T/C_l^S at $l > 2$ and hence improves sensitivity to r and n_T. The sensitivity to n_T also depends on r as shown in the previous section.

If the Universe is flat ($\Omega_0 + \Omega_\Lambda = 1$) then the cosmological constant is the only cosmological parameter that significantly affects the shape and amplitude of the
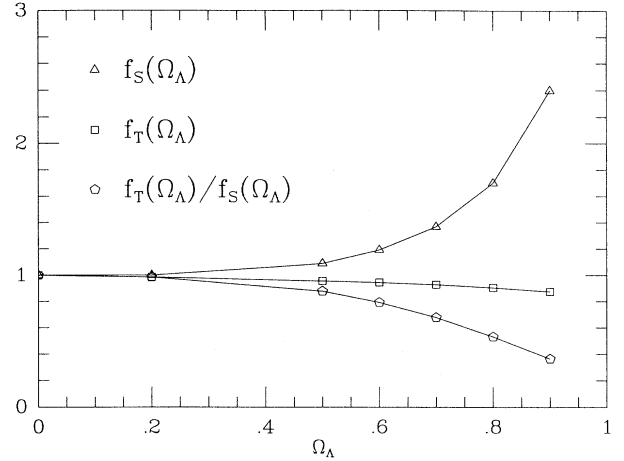
FIG. 8. Correction factors for the magnitude of the scalar and tensor quadrupoles, $f_S(\Omega_\Lambda)$ and $f_T(\Omega_\Lambda)$, as well as their ratio.

scalar spectrum for $l \lesssim 60$. As the Universe expands and becomes cosmological constant dominated, the expansion rate increases. The increased expansion rate causes the gravitational potential to decay which induces anisotropy through the integrated Sachs-Wolfe (ISW) effect[6] [37–39]. The effect is largest for wavelengths that most recently entered the horizon and hence is largest at the quadrupole. For gravitational waves, the anisotropy in the radiation is all imprinted at the last-scattering surface [24] and hence a cosmological constant has little effect.

The relationship between r and n_T is due to a relationship between the primordial tensor and scalar spectra [25]. Therefore the dependence of Q_S on Ω_Λ implies that the relationship between r and n_T also depends on Ω_Λ. Defining Ω_Λ correction factors for the scalar and tensor quadrupoles, $f_S(\Omega_\Lambda) \equiv [Q_S(\Omega_\Lambda)/Q_S(\Omega_\Lambda = 0)]^2$ and $f_T(\Omega_\Lambda) \equiv [Q_T(\Omega_\Lambda)/Q_T(\Omega_\Lambda = 0)]^2$ allows us to write the consistency relation for $\Omega_\Lambda \neq 0$:

$$r = -7 \frac{f_T(\Omega_\Lambda)}{f_S(\Omega_\Lambda)} n_T . \qquad (16)$$

The correction factors as well as their ratio are shown in Fig. 8. They were calculated numerically using the Boltzmann codes described in [28], extended to allow for a cosmological constant. The dependence of f_T/f_S on h and $\Omega_b h^2$ is much weaker.

VI. COSMIC CONFUSION

Bond *et al.* have asserted that the mapping of cosmological parameters into angular-power spectra is suffi-

---

[6]This has been called the late ISW effect by the authors of [39] to distinguish it from the early ISW effect which occurred near the last-scattering surface as the Universe was in transition from radiation domination to matter domination.

ciently degenerate that the only information we can extract from the angular-power spectrum is an amplitude and a slope. To be more precise, they claim that variations of parameters that leave $\tilde{n}$ fixed do not significantly alter the shape of the angular-power spectrum where $\tilde{n}$ is defined by [9]

$$\tilde{n} \approx n_S - 0.28\ln(1 + 0.8r) - 0.515[(1 - \Omega_\Lambda)h^2]^{1/2}$$

$$-0.00036z_R^{3/2} + 0.26 \,, \qquad (17)$$

where z_R is the redshift of reionization (effectively 0 for the standard ionization history).

This degeneracy probably does exist for any measurements that could be made by the current generation of experiments. However, here we have demonstrated that with a high-precision map one may extract not only an amplitude and a slope but also r and even to some extent the tensor index, n_T.

Is it possible to also recover h, $\Omega_b h^2$, Ω_Λ, and z_R? Hu and Sugiyama [39] have delineated the different effects of each of these parameters on the angular-power spectrum indicating that the answer is to some extent affirmative. For example, increasing $\Omega_b h^2$ not only increases the height of the first Doppler peak relative to the quadrupole (an effect that may be degenerate with n_S, Q_S, and r) but it also widens all of them. And at least for small values of h, the shape of the rise to the first Doppler peak is very sensitive to small changes in h due to the early ISW effect.

The attempt to fit the other parameters will necessarily increase to some degree the uncertainty in the inflationary parameters recovered here. The magnitude of this effect is yet to be determined. Reionization is perhaps the biggest worry. If reionization happened early enough its effects on the angular-power spectrum will not be fit by a single parameter. For these reasons the uncertainties calculated here should be understood as ideal lower limits.

For the excessively pessimistic case that we learn nothing about h, $\Omega_b h^2$, Ω_Λ, and z_R from CMB anisotropy, we can calculate the effect of these uncertainties on the inflationary observables. First we consider the confusing effect of uncertainty in $\Omega_b h^2$. Decreasing $\Omega_b h^2$ decreases the first peak at $l \simeq 200$ and leaves the trough at $l \simeq 300$ relatively unaffected. Thus a change in $\Omega_b h^2$ can be compensated for by an increase in Q_S, to fit the Doppler peak, and a decrease in n_S to fit the trough simultaneously. These shifts in Q_S and n_S create excess power at small l which is compensated for by an increase in r.

To study these shifts in the inferred values of the inflationary observables we analyzed one set of simulated data several times, each time with a different assumption about the value of Ω_b. For $\theta_{\rm FWHM} = 20$ arc min, $w = (15 \; \mu{\rm K})^{-2} \; {\rm deg}^{-2}$ we find the uncertainties in n_S and r due to uncertainties in $\Omega_b h^2$ to be

$$(\Delta n_S)_{\Omega_b h^2} \simeq 0.25\frac{\Delta(\Omega_b h^2)}{\Omega_b h^2} \,, \qquad (18)$$

$$(\Delta r)_{\Omega_b h^2} \simeq 1.3\frac{\Delta(\Omega_b h^2)}{\Omega_b h^2} \,. \qquad (19)$$

Thus $\Omega_b h^2$ must be known to better than 10% to be negligible for the measurement of r and better than 6% to be negligible for the determination of n_S.

To estimate the confusing effect of parameters other than $\Omega_b h^2$, we can use Eq. (17) which implies that

$$(\Delta n_S)_h = 0.52\sqrt{1 - \Omega_\Lambda}\Delta h = 0.23\Delta h \,, \qquad (20)$$

$$(\Delta n_S)_{\Omega_\Lambda} = \frac{0.26h}{\sqrt{1 - \Omega_\Lambda}}\Delta\Omega_\Lambda = 0.47\Delta\Omega_\Lambda \,, \qquad (21)$$

and

$$(\Delta n_S)_{z_R} = 0.016(z_R/12.4)^{3/2}\Delta z_R/z_R \,, \qquad (22)$$

where the right-most equalities hold for $h = 0.8$, $\Omega_\Lambda = 0.8$. Therefore to get to $\Delta n_S = 0.016$ we must know h to better than 0.03 for $\Omega_\Lambda = 0$ (0.07 for $\Omega_\Lambda = 0.8$) and we must know Ω_Λ to better than 0.12 for $h = 0.5$, $\Omega_\Lambda = 0$ (0.03 for $h = 0.8$, $\Omega_\Lambda = 0.8$). Clearly, if reionization occurred sufficiently early ($z_R \gtrsim 12$) its effects could be detrimental to the determination of n_S. To get anywhere near $\Delta n_S = 0.016$ in this case would probably require precise measurement of the polarization of the CMB as well.

A discussion of the prospects for precision measurements of the above parameters by means other than CMB anisotropy is beyond the scope of this paper. Clearly, given present uncertainties in cosmological parameters the uncertainty in n_S from any of the satellite experiments considered above would be "confusion dominated."

VII. DISCUSSION

Our results should be compared to those of Hinshaw et al. [40]. They simulated full-sky maps of the CMB and then analyzed small patches by finding the maximum of the likelihood function for Ω_b with all other parameters held fixed. They found, for $S/N > 1$, that sky coverage is more important than S/N and angular resolution. Angular resolution is their next most important factor; they found that $\Delta\Omega_b$ decreases by a factor of 1.3 as the beam size decreases from $1°$ to 30 arc min. Since they kept all other parameters fixed, the determination of Ω_b is effectively an amplitude determination and we can compare to our result for $\Delta Q_S^*/Q_S^*$, for which, similarly, halving the beam size causes a factor of 1.3 decrease.

This slight decrease should not, however, be used as an argument against the value of high resolution, the rewards of which are greater for the other observables. We find Δn_S and Δr are both proportional to $\theta_{\rm FWHM}$. Furthermore, it should be emphasized that even if it means reducing S/N to below unity, reducing the beam size (at fixed w) still results in dramatic improvement of our knowledge of the angular-power spectrum and the observables studied here.

Other considerations also argue for a small beam size. The extent to which the degeneracy pointed out by Bond et al. can be lifted probably depends critically on the

beam size. Also, if $\Omega + \Omega_\Lambda < 1$, the deviation of geodesics in an open Universe pushes the Doppler peak and all other features intrinsic to the last-scattering surface to smaller angles [41]. A lower limit on optimal beam size will probably come from constraints on the size of the telescope.

The total solid angle of sky over which the CMB anisotropy can be measured by a "next generation" satellite is less than 4π because of astrophysical foregrounds, mainly in the galactic plane. A more realistic value for the sky coverage is perhaps $4\pi f$ where $f = \frac{2}{3}$, which is approximately the effective CMB coverage of the COBE DMR [1]. The uncertainties calculated above scale roughly with sky coverage as $1/\sqrt{f}$.

We have seen that a full-sky map of the CMB at 20 arc min resolution with $S/N = 2$ could achieve $\Delta n_S \simeq 0.016$, $\Delta r \simeq 0.11$, and $\Delta Q_S^*/Q_S^* \simeq 0.003$. One particularly exciting prospect is the indirect detection of gravitational waves by determination of a nonzero r. While there is no generic inflationary prediction for the value of r, we note again that the simplest model gives $r = 0.28$, a number significantly different from zero. Also, many models obey the relation $r = -7(n_S - 1)$ and a slight tilt ($n_S - 1 \simeq 0.05$) is helpful in fitting the large-scale structure data. Therefore $r \simeq 0.35$ may be likely. Of course, there are also simple models that have negligibly small values of r.

The effects of uncertainty in cosmological parameters (cosmic confusion) temper our enthusiasm for the above precision. However, uncertainties in h and $\Omega_b h^2$ are likely to decrease dramatically over the next few years. Also, precision measurement of multipole moments with $l \gtrsim 300$ could possibly lift the degeneracy. Preliminary work by Spergel [13] suggests that this is indeed the case for a full-sky map with $\theta_{\rm FWHM} = 0.5°$ and $w = (10 \ \mu{\rm K})^{-2}$ deg^{-2}. It would be interesting to see how the level of degeneracy changes as the beam size and weight per solid angle are varied.

ACKNOWLEDGMENTS

APPENDIX: CALCULATION OF $\Delta C_l/C_l$

Let X_i be a Gaussian random variable with zero mean and variance σ^2. Then the sum

$$V \equiv \sum_i^n X_i^2/\sigma^2 \tag{A1}$$

is a random variable that has a χ_n^2 distribution. That is, it has probability density [42]

$$P(V)dV = \frac{V^{(n-2)/2}e^{-V/2}}{2^{n/2}\Gamma(n/2)}dV \ . \tag{A2}$$

To relate this result to the case of interest we make the identifications

$$n = 2l + 1$$

and

$$X_i = a_{lm}^{\rm map} \quad (i = 0 \to m = -l, \ i = n \to m = l) \ , \tag{A3}$$

where

$$a_{lm}^{\rm map} \equiv \sum_{j=1}^{N_{\rm pix}} \delta T_j Y_{lm}(\theta_j, \phi_j) \ . \tag{A4}$$

There are two contributions to $a_{lm}^{\rm map}$: the signal convolved with the beam $a_{lm}e^{-l^2\sigma_b^2/2}$, and the noise $a_{lm}^{\rm noise}$. These two contributions are uncorrelated. The first, by definition of C_l, has variance $C_l e^{-l^2\sigma_b^2}$. The second has covariance

$$\langle a_{lm}^{\rm noise}(a_{l'm'}^{\rm noise})^* \rangle = 4\pi \frac{\sigma_{\rm pix}^2}{N_{\rm pix}} \delta_{ll'}\delta_{mm'} \ , \tag{A5}$$

which follows from applying the rules of error propagation to the definition of $a_{lm}^{\rm map}$ and the assumption that the errors in the temperature of each pixel are uncorrelated with variance $\sigma_{\rm pix}^2$. Thus we make the further identification

$$\sigma^2 \equiv \langle |a_{lm}^{\rm map}|^2 \rangle = C_l e^{-l^2\sigma_b^2} + 4\pi \frac{\sigma_{\rm pix}^2}{N_{\rm pix}} \tag{A6}$$

since that is the total variance of $a_{lm}^{\rm map}$.

To estimate C_l from $C_l^{\rm map} \equiv \sum_m |a_{lm}^{\rm map}|^2/(2l + 1)$ we must subtract off the expected noise contribution and correct for the finite width of the beam. Therefore

$$C_l^{\rm est} = \left(C_l^{\rm map} - 4\pi \frac{\sigma_{\rm pix}^2}{N_{\rm pix}} \right) e^{l^2\sigma_b^2} \ . \tag{A7}$$

Since the weight-per-solid angle is $w \equiv (\sigma_{\rm pix}^2 \Omega_{\rm pix})^{-1} = \left(\frac{4\pi\sigma_{\rm pix}^2}{N_{\rm pix}} \right)^{-1}$,

$$C_l^{\rm est} = (C_l^{\rm map} - w^{-1})e^{l^2\sigma_b^2} \ . \tag{A8}$$

From this it follows that

$$V = (2l + 1)\frac{C_l^{\rm est} + w^{-1}e^{l^2\sigma_b^2}}{C_l + w^{-1}e^{l^2\sigma_b^2}} \ , \tag{A9}$$

and therefore

$$P(C_l^{\rm est})dC_l^{\rm est} = P(V)\frac{dV}{dC_l^{\rm est}}dC_l^{\rm est}$$
$$= \frac{n}{C_l + w^{-1}e^{l^2\sigma_b^2}} \frac{V^{(n-2)/2}e^{-V/2}}{2^{n/2}\Gamma(n/2)}dC_l^{\rm est} \ , \tag{A10}$$

where $n \equiv 2l + 1$. With the probability density for $C_l^{\rm est}$ in hand, it is easy to show that $\langle C_l^{\rm est} \rangle = C_l$ and

$$\langle (C_l^{\rm est} - C_l)(C_{l'}^{\rm est} - C_{l'}) \rangle$$
$$= \frac{2}{2l + 1}(C_l + w^{-1}e^{l^2\sigma_b^2})^2\delta_{ll'} \ . \tag{A11}$$

[1] G. F. Smoot *et al.*, Astrophys. J. **396**, L1 (1992).

[2] A reasonably complete and current list of temperature anisotropy detections and upper limits: C. L. Bennett *et al.*, Astrophys. J. **436**, 423 (1994); K. Gorski *et al.*, *ibid.* **430**, L89 (1994) (COBE DMR 2-yr data); K. Ganga *et al.*, *ibid.* **410**, L57 (1993) (FIRS); S. Hancock *et al.*, Nature (London) **367**, 333 (1995) (Tenerife); T. Gaier *et al.*, Astrophys. J. **398**, L1 (1992); J. Schuster *et al.*, *ibid.* **412**, L47 (1993) (SP91); J. Gundersen *et al.*, *ibid.* **443**, L57 (1995) (SP94); E. J. Wollack *et al.*, *ibid.* **419**, L49 (1993); C. B. Netterfield *et al.*, *ibid.* **445**, L69 (1995) (Saskatoon or Big Plate); P. Meinhold and P. Lubin, *ibid.* **370**, L11 (1991) (SP89); P. de Bernardis *et al.*, *ibid.* **422**, L33 (1994) (ARGO); M. Dragovan *et al.*, *ibid.* **355**, L67 (1994) (PYTHON); P. Meinhold *et al.*, *ibid.* **409**, L1 (1993); J. Gundersen *et al.*, *ibid.* **413**, L1 (1993) (MAX3); M. Devlin *et al.*, *ibid.* **430**, L1 (1994); A. Clapp *et al.*, *ibid.* **433** L57 (1994) (MAX4); E. S. Cheng *et al.*, *ibid.* **420**, L37 (1993) (MSAM); G. S. Tucker *et al.*, *ibid.* **419**, L45 (1993) (White Dish); A. C. S. Readhead *et al.*, *ibid.* **346**, L56 (1989) (Owens Valley).

[3] D. T. Wilkinson, in *Proceedings of the Ninth Lake Louise Winter Institute: Particle Physics and Cosmology*, edited by A. Astbury, B. A. Campbell, W. Israel, F. C. Khana, D. Page, and J. L. Pinfold (World Scientific, New Jersey, 1995).

[4] For a review of the current observations from the perspective of inflation, see P. J. Steinhardt, in *Proceedings of the 1994 Snowmass Summer Study: Particle and Nuclear Astrophysics and Cosmology in the Next Millenium*, edited by E. W. Kolb and R. Peccei (World Scientific, Singapore, 1995). Two other recent reviews of CMB anisotropy are M. White, D. Scott, and J. Silk, Annu. Rev. Astron. Astrophys. **32**, 319 (1994); J. R. Bond, in *Proceedings of the IUCAA Dedication Ceremonies*, edited by T. Padmanabhan (Wiley, New York, 1993).

[5] For an optimistic view on the existence of a Doppler peak, see D. Scott and M. White, in *Proceedings of the CWRU CMB Workshop: Two Years After COBE*, edited by L. Krauss and P. Kernan (World Scientific, New York, 1995).

[6] P. J. E. Peebles, Nature (London) **327**, 210 (1987); Astrophys. J. **315**, L73 (1987).

[7] W. Hu, E. F. Bunn, and N. Sugiyama, Astrophys. J. **447**, L59 (1995).

[8] U. Pen, D. Spergel, and N. Turok, Phys. Rev. D **49**, 692 (1994); D. P. Bennett, A. Stebbins, and F. Bouchet, Astrophys. J. **399**, L5 (1992); D. P. Bennett and S. H. Rhie, *ibid.* **406**, L7 (1993). For defects in an open universe see U. Pen and D. Spergel, Phys. Rev. D **51**, 4099 (1995).

[9] J. R. Bond *et al.*, Phys. Rev. Lett. **72**, 13 (1994).

[10] S. Dodelson, L. Knox, and E. W. Kolb, Phys. Rev. Lett. **72**, 3444 (1994).

[11] S. Dodelson and A. Kosowsky, Phys. Rev. Lett. **75**, 604 (1995).

[12] S. Meyer, G. Smoot, and E. Wright, in *Proceedings of the 1994 Snowmass Summer Study* [4].

[13] D. N. Spergel (unpublished).

[14] For the generation of scalar perturbations see A. H. Guth and S. Y. Pi, Phys. Rev. Lett. **49**, 1110 (1982); S. W. Hawking, Phys. Lett. **115B**, 295 (1982); A. A. Starobinskii, *ibid.* **117B**, 175 (1982); J. M. Bardeen, P. J. Steinhardt, and M. S. Turner, Phys. Rev. D **28**, 697

(1983). For the generation of tensor perturbations see V. A. Rubakov, M. Sazhin, and A. Veryaskin, Phys. Lett. **115B**, 189 (1982); R. Fabbri and M. Pollock, *ibid.* **125B**, 445 (1983); A. A. Starobinskii, Sov. Astron. Lett. **9**, 302 (1983); L. Abbott and M. Wise, Nucl. Phys. **B244**, 541 (1984).

[15] A. D. Linde, Phys. Lett. **129B**, 177 (1983).

[16] A. Kosowsky and M. S. Turner, Phys. Rev. D **52**, 1739 (1995).

[17] For a recent review, see C. J. Copi, D. N. Schramm, and M. S. Turner, Science **267**, 192 (1995).

[18] A. Songaila, L. L. Cowie, C. J. Hogan, and M. Rugers, Nature (London) **386**, 599 (1994); R. F. Carswell, M. Rauch, R. J. Weymann, A. J. Cooke, and J. K. Webb, Mon. Not. R. Astron. Soc. (to be published).

[19] W. Freedman *et al.*, Nature (London) **371**, 757 (1994).

[20] B. P. Schmidt *et al.*, Astron. J. **107**, 1444 (1994).

[21] R. Crittenden, R. Davis, and P. Steinhardt, Astrophys. J. **417**, L13 (1993); R. A. Frewin, A. G. Polnarev, and P. Coles, Mon. Not. R. Astron. Soc. **266**, L21 (1994).

[22] S. M. Carroll, W. H. Press, and E. L. Turner, Annu. Rev. Astron. Astrophys. **30**, 499 (1992).

[23] R. Bar-Kana, Phys. Rev. D **50**, 1157 (1994).

[24] M. S. Turner, M. White, and J. E. Lidsey, Phys. Rev. D **48**, 4613 (1993).

[25] E. J. Copeland, E. W. Kolb, A. R. Liddle, and J. E. Lidsey, Phys. Rev. Lett. **71**, 219 (1993); Phys. Rev. D **48**, 2529 (1993); M. S. Turner, *ibid.* **48**, 3502 (1993); A. Liddle and D. Lyth, Phys. Lett. B **291**, 391 (1992); R. Davis *et al.*, Phys. Rev. Lett. **69**, 1856 (1992).

[26] E. F. Bunn, D. Scott, and M. White, Astrophys. J. **441**, L9 (1995).

[27] L. Knox and M. S. Turner, Phys. Rev. Lett. **73**, 3347 (1994).

[28] The scalar angular-power spectrum calculation is described in S. Dodelson and J. M. Jubas, Phys. Rev. Lett. **70**, 2224 (1993); the tensor is described in [10]. Also see J. R. Bond and G. Efstathiou, Mon. Not. R. Astron. Soc. **226**, 255 (1987).

[29] See, e.g., L. Abbott and M. Wise, Astrophys. J. **282**, L47 (1984).

[30] L. Danese *et al.*, Astrophys. Lett. Comm. (to be published).

[31] W. N. Brandt *et al.*, Astrophys. J. **424**, 1 (1994).

[32] S. Dodelson and A. Stebbins, Astrophys. J. **433**, 440 (1994).

[33] Gary Hinshaw (personal communication).

[34] To model the foregrounds more realistically would require a much greater effort along the lines of the work by Bouchet *et al.* They are simulating multifrequency maps, which include CMB and many different foreground contaminants, to aid in the design of SAMBA. For a brief report on their plans see F. R. Bouchet *et al.*, in *Far Infrared and Sub-millimeter Space Missions in the Next Decade*, edited by M. Sauvage (Space Science Review, Paris, France, in press).

[35] W. H. Press, S. A. Teukolsky, W. T. Vetterling, and B. P. Flannery, *Numerical Recipes*, 2nd ed. (Cambridge University Press, Cambridge, England, 1993).

[36] E. W. Kolb and S. Vadas, Phys. Rev. D **50**, 2479 (1994). Equation (15) appears in A. Liddle and M. S. Turner, *ibid.* **50**, 758 (1994).

[37] L. Kofman and A. Starobinsky, Sov. Astron. Lett. **11**,

271 (1986).

[38] K. M. Gorski, J. Silk, and N. Vittorio, Phys. Rev. Lett. **68**, 733 (1992).

[39] W. Hu and N. Sugiyama, Astrophys. J. **444**, 489 (1995); Phys. Rev. D **51**, 2599 (1995).

[40] G. Hinshaw, C. L. Bennett, and A. Kogut, Astrophys. J. **441**, L1 (1995).

[41] M. Kamionkowsky, B. Ratra, D. N. Spergel, and N. Sugiyama, Astrophys. J. **434**, L1 (1994); N. Sugiyama and N. Gouda, Prog. Theor. Phys. **88**, 803 (1992).

[42] P. J. Bickel and K. A. Doksum, *Mathematical Statistics: Basic Ideas and Selected Topics* (Holden-Day, San Francisco, 1977).